Sub-band Energy Based Collaborative Target Localization in Wireless Sensor Network System

Xiaohong Sheng, and Yu-Hen Hu
Email: sheng@ece.wisc.edu,hu@engr.wisc.edu,
http://www.ece.wisc.edu/∼sensit

Abstract

In this paper, sub-band energy based collaborative target localization in wireless sensor network is presented. Three steps including target detection, target location candidates estimation and target location identification have been performed to realize the task of target localization. In the step of target detection, each sensor node detects the targets by filtered total acoustic energy based constant false alarm (*FTE CFAR*) detector, acoustic sub-band energy based constant false alarm (*SE CFAR*) detector and multi-modality energy based constant false alarm (*MME CFAR*) detector respectively. Region based target detection fusion is then performed based on all node detection results from the three detectors. Sub-band acoustic energy based algorithm is performed as the second step to estimate the target location candidates when targets are detected in the region. Finally, sequential bayesian estimation is used to identify the most possible target location from these candidate locations. Experiments have been conducted. Results show that this new approach is accurate and robust to the strong background noise. Besides, communication bandwidth and computation burden are not high compared with the other approaches.

I. Introduction

The emergence of small, low-power devices that integrate micro-sensing and actuation with on-board processing and wireless communication capabilities stimulates great interests in wireless distributed sensor network. Such distributed sensor network systems have a variety of applications [1], [2]. Examples include underwater acoustics, battlefield surveillance, electronic warfare, geophysics, seismic remote sensing, and environmental monitoring. Such sensor networks are often designed to perform tasks such as detection, classification, localization and tracking of one or more targets in the sensor field. The sensors are typically battery-powered and have limited wireless communication bandwidth. Therefore, efficient collaborative signal processing algorithms that consume less energy for computation and communication are needed.

An important collaborative signal-processing task is source localization using a passive and stationary sensor network. The objective is to estimate the positions of the moving targets within a sensor field monitored by the sensor network.

Most localization methods depend on three types of physical variables measured by or derived from sensor readings for localization: time delay of arrival (TDOA), direction of arrival (DOA) and received sensor signal strength or power. DOA can be estimated by exploiting the phase difference measured at receiving sensors [3], [4],[5] and is applicable in the case of a coherent, narrow band source. TDOA is suitable for broadband source and has been extensively investigated [6], [7], [8]. In practice, DOA measurement typically require costly antenna array on each node. The TDOA techniques require a high demand on the accurate measurement or estimation of time delay. In contrast, received sensor signal strength is comparatively much easier and less costly to obtain from the time series recordings from each sensor.

In [9], source localization based on the received acoustic power (energy) has been presented. Simulations and experiments show that this approach is robust and accurate most of time. However, the performance of this approach degrades a lot when source signals are corrupted by strong background noise. To address these problems, we propose a new approach that uses sub-band energy rather than the entire energy to localize the targets.

This project is supported by DARPA under grant no. F 30602-00-2-0555

Acoustic sub-band energy distribution or say, power spectrum density distribution (*PSD*) is a feature of a particular target. Background noise may have significant components on some spectrum covered by the target signal, but it is not necessary that background noise has significant components on all the spectrum covered by the target signal. Therefore, if we estimate the target location based on the different sub-band energies, we may get several location candidates, some of these location candidates should be the true target location since these locations are estimated from un-corrupted sub-band energy decay functions. We would like to identify the true target location from these location candidates. Using sequential bayesian detection, we can identify this true target location.

The task of localization is divided into three steps, i.e., target detection by node detection using *FTE CFAR* detector, *SE CFAR* detector and *MME CFAR* detector and region based decision fusion based on the node detection results; target candidate location estimation using sub-band acoustic energies when targets are detected in the region and sequential bayesian detection to identify the true target location. The first step: target detection is important. It can reduce the computation burden since localization algorithm won't be executed if there is no detection. Besides, it makes the localization algorithm more robust since when targets are detected in the region, we may have higher SNR, which is an important condition for high performance of all localization algorithms.

Experiments are conducted to evaluate this collaborative target localization algorithm in wireless sensor network system. Results show that this new approach is accurate and robust to the strong background noise.

The rest of the paper is organized as follows: In section II, we introduce node detection using *FTE CFAR* detector, *SE CFAR* detector and *MME CFAR* detector and region based decision fusion based on the node detection results. In section III, we introduce sub-band energy based source localization algorithm. Sequential bayesian detection to identify the true target location is introduced in section IV. Experiments and evaluations on this approach are provided in section V. A conclusion is given is section VI.

II. Target detection in wireless sensor network

The sensor field is divided into several smaller region. Each region, we define one manager sensor node. Other nodes are defined as the detection nodes.

The region is activated by our tracking algorithm implemented by Kalman filter, which uses the previous localization results to predict the target location in the next time period. When it predicts that the targets will go into another region, the current region manager node will send this information to the manager node of that region. The corresponding region is then activated. Each detection node in the new activated region will perform the node detection using filtered total acoustic energy based constant false alarm (*FTE CFAR*) detector, acoustic sub-band energy based constant false alarm (*SE CFAR*) detector and multi-modality energy based constant false alarm (*MME CFAR*) detector. Each detection node will send these results to the manager node. Manager node will then perform region based fusion decision to detect the target in the region.

A. *Energy-Based* CFAR *Detector*

Energy based constant false alarm (*CFAR*) detector detects targets based on the assumption that background noise is relatively stable. When signal energy received by the sensor exceeds certain value, we assume that the target appears. The algorithm is proceeded as follows:

A t_0 time series is taken at the beginning to initialize the mean $\mu_i(0)$ and standard deviation $\sigma_i(0)$ of the background noise energy, assuming no presence of target during this period. This is known as the noise level initialization phase. Then each node i goes to the detection phase where the energy $y_i(n)$ is compared to a threshold $T_i(n)$ at time n. Assuming the noise energy sequence is independent Gaussian, we can define $T_i(n)$ as $T_i(n) = \mu_i(n) + C\sigma_i(n)$, where C is a constant chosen to yield a desired constant false alarm probability:

$$P_{FA} = \frac{1}{\sqrt{(2\pi)}} \int_C^\infty exp(-\frac{1}{2}u^2)du$$

The decision $\gamma_i(n)$ then is

$$\gamma_i(n) = \begin{cases} 1 & y_i(n) > T_i(n) \\ 0 & y_i(n) < T_i(n) \end{cases}$$

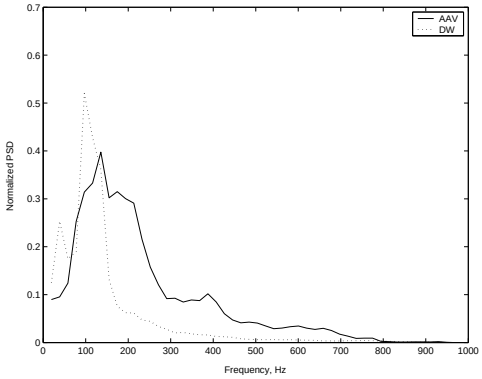

Fig. 1. Sub-band acoustic energy distribution for AAV and DW

where $\gamma_i(n) = 1$ indicates the target presence at time n and 0 for target absence at time n. If $\gamma_i(n) = 1$, then the threshold keeps unchanged, $T_i(n) = T_i(n-1)$; otherwise, it is updated as follows:

$$\mu_i(n) = (1-\alpha)\mu_i(n-1) + \alpha y_i(n)$$

$$\sigma_i^2(n) = (1-\alpha)\sigma_i^2(n-1) + \alpha[y_i(n) - \mu_i(n)]^2$$

$$T_i(n) = \mu_i(n-1) + C\sigma_i(n)$$

where α is a factor between 0 and 1, indicating the approximate inverse of average length of mean and variance. For example, $\alpha = 1/8$ indicates the average length is 8. The reason we use this factor is to avoid the recording of the previous raw signal so that we can save memory and computation time, but still get the approximate updated mean and variance of the noise.

As we point out in the beginning, energy based *CFAR* detector detects the targets by assuming background noise is relatively stable. However, in real situation, there are various sources that are not the targets we are detecting. Total energy based *CFAR* detector will treat them as real targets and produce false alarm. Following we will introduce filtered total acoustic energy based constant false alarm (*FTE CFAR*) detector, acoustic sub-band energy based constant false alarm (*SE CFAR*) detector and multi-modality energy based constant false alarm (*MME CFAR*) detector to reduce the false alarm.

B. FTE CFAR *Detector,* SE CFAR *Detector and* MME CFAR *Detector*

Acoustic power spectrum density (*PSD*) distribution (sub-band energy distribution) is a feature for a particular target. For example, acoustic energy for Assault Amphibian Vehicle (AAV) is mainly distributed on the frequency between $0HZ$ and $500HZ$; acoustic energy for dragon wagon vehicle (DW) is mainly distributed on the sub-band between $0HZ$ and $200HZ$. Fig. 1 shows the *PSD* distribution for AAV and DW acoustic signal averaged by measurements of 17 nodes in 2 minutes in our experiment. The sampling frequency is 4960HZ.

As described previously, the acoustic signal received by the sensor node might be corrupted by any sources that we are not interested. The existence of these spurious sources degrades the performance of our detection and localization. In this paper, we treat all these spurious sources as well as random noise as background noise. An important task in detection and localization algorithm is to filter out background noise energies from received energy. One way to do this is to analyze the measured sub-band energy and use sub-band energy distribution characteristics to do detection and localization. In this section, we will introduce *FTE CFAR* detector, *SE CFAR* detector and *MME CFAR* detector to filter out the background noise in the target detection. In section III, we will introduce how to improve the localization results by sub-band energy based localization algorithm.

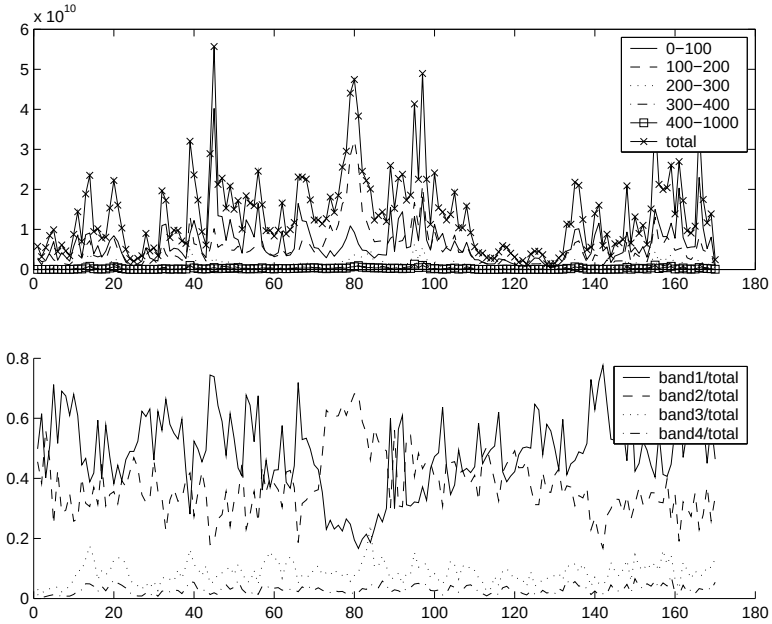

Fig. 2. Measured energy distribution for AAV by sensor node 61

1) FTE CFAR *Detector:* Fig. 2 shows total energy, sub-band energies and ratios of sub-band energy to total energy measured by one node in our experiment for detecting AAV targets. The sampling speed is 4960HZ. The energy is calculated by averaging the time window of 0.75 second, i.e., by averaging non-overlapping 3720 sampling points. It can be seen that the total energy is quite noisy. If we use total energy for *CFAR* node detection, detection results have quite a few of false alarms. Yet, the figure also shows that only the points at the interval between 72(0.75*72sec) and 88(0.75*88sec) have the sub-band energy distribution (or PSD distribution) similar to AAV sub-band energy distribution, i.e., sub-band energy in the range of $100 \sim 200HZ$ has the largest component in the total energy, sub-band energy in the range of $0 \sim 100HZ$ has the second largest component, the third largest component is the range from 200HZ to 300HZ and so on. So, with the comparison of measured sub-band energy distribution and sub-band energy distribution characteristics for the detecting target, we can filter out a large amount of false alarm. We call this algorithm as filtered total energy based CFAR detector (*FTE CFAR*).

2) SE CFAR *Detector: FTE CFAR* detector can reduce lots of fault alarm. Yet, it also creates the probability of miss detection. It is possible that there exist several sources in the detection region, one of which is the target source we are detecting, but this target signal strength is not as strong as other sources, or it is relatively far to the detection node compared to the other sources. Then if we use total energy based *CFAR* detector, we can detect this target. However, if we use *FTE CFAR* detector, we will miss detecting the targets as the sub-band energy distribution is no longer to be similar to that particular target and so, the detection will be filtered out. To reduce the probability of miss detection, we also detect the targets by using sub-band energy based CFAR (*SE CFAR*) detector. The *SE CFAR* detection results are then fused with *FTE CFAR* detection results. The use of *SE CFAR* detection is hinted by the following observation:

For every target, its acoustic signal is band limited, i.e., its acoustic energy is mainly concentrated on certain bands. Background noise may have significant components on some spectrum covered by the target signal, but it is not necessary that background noise has significant components on all the spectrum of the target signal. Therefore, if targets exist in the region, even if the signal is corrupted, there still exists some relatively clean bands that are mainly comprised of the target signal only. We can use sub-band energy to detect the target and use these detection results to compensate the *FTE CFAR* detection results. For example, in Fig. 2, background noise is mainly from 0HZ to 100HZ. It completely destroyed the target signal at the sub-bands of this range. However, it shouldn't destroy the sub-band from 100HZ to 500HZ, which also have the significant components for AAV signal. So, if it is purely noise signal, then we get 1 detection at the sub-band from 0Hz

to 100 Hz, but 0 detection at the sub-bands from 100HZ to 500HZ and 0 detection of *FTE CFAR* detection results. Use certain fusion decision, we announce 0 detection. If it is strong noise plus true target, we get 0 detection of *FTE CFAR* (as the noise destroyed the spectrum distribution), however, we get 1 detection at all the sub-bands from 0Hz to 500Hz, use certain fusion algorithm, we can still detect the target.

The choices of the sub-band ranges depend on the *PSD* distribution characteristics of the detected signal. For example, the energy of acoustic signal for AAV is mainly concentrated on $0HZ \sim 500HZ$, we can choose the sub-band components for AAV as $0 \sim 100HZ$, $100 \sim 200HZ$, $200 \sim 300HZ$, $300 \sim 400HZ$ and $400 \sim 500HZ$. For DW, we can choose the sub-band components as $0 \sim 40HZ$, $40 \sim 80HZ$, $80 \sim 120HZ$, $120 \sim 160HZ$ and $160 \sim 200HZ$ since the acoustic signal for DW is mainly concentrated on the sub-band from 0HZ to 200HZ.

3) MME CFAR *Detector:* To further reduce the false alarm and miss detection, we also use the multi-modality signal such as seismic and PIR signal to do the energy based CFAR (*MME CFAR*) detection.

The overall strategy of node detection is as follows:

For every node i,

1. Detect the target use total acoustic energy, if it is detected, set $AD_{i0} = 1$, where i stands for the i^{th} sensor node, 0 stands for the detection from total energy, AD stands for the acoustic detection.

2. If $AD_{i0} = 1$, check the spectrum distribution. If the spectrum distribution is similar to the spectrum distribution of the target we are detecting, don't change the set of AD_{i0}, otherwise, set $AD_{i0} = 0$; (Here, we just compare the ranking of the measured sub-band energy components with the ranking of the sub-band energy components of the detecting target. If the ranking of measured energy components is the same as the ranking of the particular target sub-band energy component, we treat it as similar; otherwise, we treat it as non-similar).

3. For sub-band j, use *SE CFAR* detector to detect the target based on the sub-band j's energy, and get the detection result AD_{ij}, $j = 1, 2, ...M$. M is the number of sub-band we choose for *SE CFAR* detection.

4. Detecting the target based on other modality energy, such as seismic energy or PIR energy respectively, and get the detection results SD_i and PD_i.

5. Node i sends AD_{ij} and SD_i, PD_i to the manager node for all j. Manager node will use certain fusion algorithm to fuse all these detection results.

C. Region Fusion Detection

In above, we introduced *FTE CFAR* detection, *SE CFAR* detection and *MME CFAR* detection. In this section, we will describe how manager node uses these node detection results to perform region based target detection.

The manager node first uses majority voting to get the detection results for each modality and each acoustic sub-band detection. For example, in region 1, if there are more than N/2 nodes report *FTE CFAR* detection, where N is the number of detection node in region 1, the manager node judges that *FTE CFAR* detection for region 1 is 1. Similarly, for acoustic sub-band j detection, suppose there are less than N/2 nodes report detection, manager node considers the acoustic sub-band j detection in this region is 0. So does seismic modality detection. PIR sensor is special, manager node announces PIR detection if there is more than 1 PIR detection. After that, manager node uses different weights for different modality and different sub-band acoustic energy to fuse their detection results. If the fusion result announces that targets are in the region, acoustic localization algorithm is activated and performed to further locate the targets in the region. Fig. 3 shows the overall picture of region based fusion detection.

III. Acoustic Sub-band Energy Based Source Localization

Localization algorithm is executed when targets are detected in the region. In this section, we will describe acoustic sub-band energy based source localization algorithm.

In [9], it is derived that, when sound propagates in free and homogenous space and the targets are pre-detected to be in a certain region of the sensor field, the acoustic energy decay function can be modelled by the following equation:

$$y_i(n) = y_{si}(n) + \varepsilon_i(n) = g_i \sum_{j=1}^{K} \frac{S_j(n)}{\parallel \boldsymbol{\rho}_j(n) - \mathbf{r}_i \parallel^2} + \varepsilon_i(n) \tag{1}$$

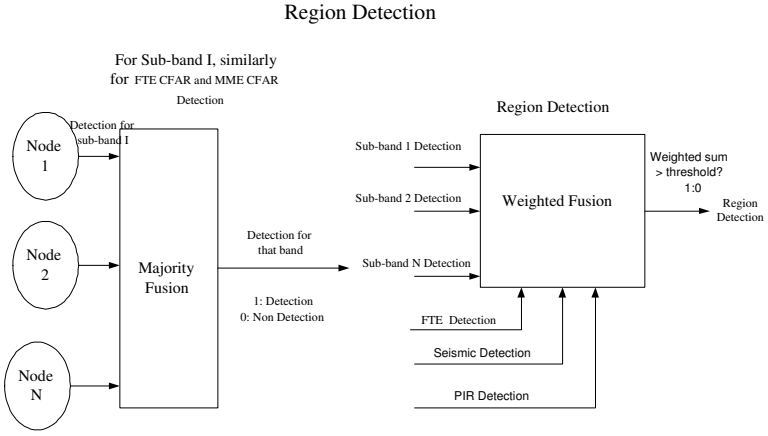

Fig. 3. Flowchart of region fusion detection based on the three node detectors

Where K is the number of targets detected in the region. $y_i(n)$ is the acoustic energy received by the i^{th} sensor. $y_{si}(n)$ is the the sum of the decayed energy emitted from each of these K targets to i^{th} sensor (i.e. energy sources). $\varepsilon_i(n)$ is a perturbation term that summarizes the net effects of background additive noise and the parameter modelling error. g_i and $\mathbf{r}_i$ are the gain factor and location of the i^{th} sensor, $S_j(n)$ and $\boldsymbol{\rho}_j(n)$ are respectively, the energy emitted by the j^{th} source (measured at 1 meter from the source) and its location during n^{th} time interval. N is the number of sensors in the activated region, p is the location dimension.

The probability distribution of $\varepsilon_i(n)$ can be modelled well with an independently, identically distributed Gaussian random variable when the time window T for averaging the energy is sufficiently large, i.e, $T > 40/f_s$, where f_s is the sampling frequency [9]. The mean and variance of each $\varepsilon_i(n)$, denoted by $\mu_i(n)\,(>0)$ and $\sigma_i^2(n)$, can be empirically estimated from our *CFAR* detector that we described previously.

*A. Maximum Likelihood (*ML*) Estimation with Projection Solution*

Define

$$\mathbf{Z} = \left[\begin{array}{cccc} \frac{y_1-\mu_1}{\sigma_1} & \frac{y_2-\mu_2}{\sigma_2} & \cdots & \frac{y_N-\mu_N}{\sigma_N} \end{array} \right]^{\Gamma} \tag{2}$$

Equation (1) can be simplified as:

$$\mathbf{Z} = \boldsymbol{GDS}+\boldsymbol{\xi} = \boldsymbol{HS}+\boldsymbol{\xi} \tag{3}$$

Where:

$$\mathbf{S} = \left[\begin{array}{ccc} S_1 & S_2 & \cdots S_K \end{array} \right]^{\Gamma} \tag{4}$$

$$\mathbf{H} = \mathbf{GD} \tag{5}$$

$$\mathbf{G} = diag \left[\begin{array}{cccc} \frac{g_1}{\sigma_1} & \frac{g_2}{\sigma_2} & \cdots & \frac{g_N}{\sigma_N} \end{array} \right] \tag{6}$$

$$\mathbf{D} = \left[\begin{array}{cccc} \frac{1}{d_{11}^2} & \frac{1}{d_{12}^2} & \cdots & \frac{1}{d_{1K}^2} \\ \frac{1}{d_{21}^2} & \frac{1}{d_{22}^2} & \cdots & \frac{1}{d_{2K}^2} \\ \vdots & \vdots & \ddots & \vdots \\ \frac{1}{d_{N1}^2} & \frac{1}{d_{N2}^2} & \cdots & \frac{1}{d_{NK}^2} \end{array} \right] \tag{7}$$

$d_{ij} = |\boldsymbol{\rho}_j - \mathbf{r}_i|$ is the Euclidean distance between the i^{th} sensor and the j^{th} source.
$\boldsymbol{\xi} = [\xi_1\, \xi_2 \ldots \xi_N]^T$, where ξ_i is independent Gaussian noise $\sim N(0,1)$

The unknown parameters $\boldsymbol{\theta}$ in the above function is:

$$\boldsymbol{\theta} = \begin{bmatrix} \boldsymbol{\rho}_1^T & \boldsymbol{\rho}_2^T & \cdots & \boldsymbol{\rho}_K^T & S_1 & S_2 & \cdots & S_K \end{bmatrix}^T$$

The log-likelihood function is:

$$\ell(\boldsymbol{\theta}) = \frac{-1}{2} \parallel \mathbf{Z} - \mathbf{GDS} \parallel^2 \tag{8}$$

Given the log-likelihood function $\ell(\boldsymbol{\theta})$ denoted as equation (8), *ML* estimations of the parameters $\boldsymbol{\theta}$ are the values that maximize $\ell(\boldsymbol{\theta})$, or equivalently, minimize

$$Ł(\boldsymbol{\theta}) = \parallel \mathbf{Z} - \mathbf{GDS} \parallel^2 \tag{9}$$

Equation (9) has $K(p+1)$ unknown parameters, there must be at least $K(p+1)$ or more sensors reporting acoustic energy readings to yield an unique solution to this nonlinear least square problem.

Define pseudoinverse of $\mathbf{H}$ as $\mathbf{H}^\dagger$, projection matrix of $\mathbf{H}$ as $\mathbf{P}_H$, and perform reduced SVD of $\mathbf{H}$, we have:

$$\mathbf{H}^\dagger = \left(\mathbf{H}^T\mathbf{H}\right)^{-1}\mathbf{H}^T \tag{10}$$

$$\mathbf{P}_H = \mathbf{H}(\mathbf{H^T H})^{-1}\mathbf{H^T} = \mathbf{U_H}\,\mathbf{U_H^T} \tag{11}$$

$$\mathbf{H} = \mathbf{GD} = \mathbf{U}_H\boldsymbol{\Sigma}_H\mathbf{V}_H^T \tag{12}$$

Set $\frac{\partial \mathbf{L}}{\partial \mathbf{S}} = 0$, we have:

$$\mathbf{S} = \mathbf{H}^\dagger\mathbf{Z} \tag{13}$$

Insert (13) into the cost function (9), we get modified cost function as follows:

$$\begin{aligned} \underbrace{\arg\text{MIN}}_{\{\rho_1,\rho_2,\ldots\rho_k\}} L &= \underbrace{\arg\text{MIN}}_{\{\rho_1,\rho_2,\ldots\rho_k\}} \left(\mathbf{Z}^T(\mathbf{I}-\mathbf{P}_H)^T(\mathbf{I}-\mathbf{P}_H)\mathbf{Z}\right) \\ &= \underbrace{\arg\text{MAX}}_{\{\rho_1,\rho_2,\ldots\rho_k\}} \left(\mathbf{Z}^T\mathbf{P}_H^T\mathbf{Z}\right) = \underbrace{\arg\text{MAX}}_{\{\rho_1,\rho_2,\ldots\rho_k\}} \mathbf{Z}^T\mathbf{U}_H\mathbf{U}_H^T\mathbf{Z} \end{aligned} \tag{14}$$

For single source, $j = 1$,

$$\mathbf{H} = \left[\frac{g_1}{\sigma_1\, d_1^2}, \frac{g_2}{\sigma_2\, d_2^2}, \cdots, \frac{g_n}{\sigma_n\, d_n^2}\right]^T,$$

$$\mathbf{U_H} = \frac{\mathbf{H}}{\parallel \mathbf{H} \parallel}$$

Exhaustive search can be used to get the source location to maximize function (14). However, the computation complexity is very high. For example, suppose our detected search region is 128×128, if we use *exhaustive* search using the grid size of 4×4, we need 1024^K times of search for every estimation point, where K is the number of the targets. Rather, we can use Multi-Resolution (*MR*) search to reduce the number of search times. For example, we can use the search grid size 16×16, 8×8, 4×4 sequentially. Then, the number of search times is reduced to $64^K + 2 * 4^K$. For two targets, it needs 4128 search times using *MR* search with this search strategy and 1024^2 search times using *exhaustive* search to get one estimation. We can further reduce the number of search times by reducing our search region based on the previous location estimation, the time interval between two localization operation, possible vehicle speed and estimation error. In our experiment, all these conditions are used. The search area we used for the *projection* solution is $(x_i - 32, x_i + 32) \times (y_i - 32, y_i + 32)$, where (x_i, y_i) is the previous estimation location of the i^{th} target. Therefore, for single target, we need only 24 search; for two targets, we need 288 search for every localization estimation, which is feasible for our distributed wireless networking system.

B. Nonlinear Least Square (NLS) Estimation for single Target Localization

When there is only one target in the region, by ignoring the additive noise term ε_i in the equation (1), we can compute the energy ratio φ_{ij} of the i^{th} and the j^{th} sensors as follows:

$$\varphi_{ij} = \left(\frac{y_i/y_j}{g_i/g_j}\right)^{-1/2} = \frac{\parallel \boldsymbol{\rho} - \mathbf{r}_i \parallel}{\parallel \boldsymbol{\rho} - \mathbf{r}_j \parallel} \tag{15}$$

Here $\boldsymbol{\rho}$ denotes the single target location. Other parameters are the same as what described before.

Note that by sorting the calibrated energy readings y_i/g_i, for $0 < \varphi_{ij} \neq 1$, all the possible source coordinates $\boldsymbol{\rho}$ that satisfy equation (15) reside on a p-dimensional hyper-sphere described by the equation:

$$\parallel \boldsymbol{\rho} - \mathbf{c}_{ij} \parallel^2 = \zeta_{ij}^2 \tag{16}$$

Where the center $\mathbf{c}_{ij}$ and the radius ζ_{ij} of this hyper-sphere associated with sensor i and j are given by:

$$\mathbf{c}_{ij} = \frac{\mathbf{r}_i - \varphi_{ij}^2 \mathbf{r}_j}{1 - \varphi_{ij}^2},\ \zeta_{ij} = \frac{\varphi_{ij} \parallel \mathbf{r}_i - \mathbf{r}_j \parallel^2}{1 - \varphi_{ij}^2} \tag{17}$$

If $\varphi_{ij} = 1$, the solution of equation (15) form a hyper-plane between $\mathbf{r}_i$ and $\mathbf{r}_j$, i.e.:

$$\boldsymbol{\rho}(t)\boldsymbol{\iota}_{ij} = \tau_{ij} \tag{18}$$

Where $\boldsymbol{\iota}_{ij} = \mathbf{r}_i - \mathbf{r}_j$, $\tau_{ij} = \frac{|\mathbf{r}_i|^2 - |\mathbf{r}_j|^2}{2}$

So far, we show that, for single target at noiseless situation, each energy ratio dictates that the potential target location must be on a hyper-sphere or a hyper-plane within the sensor field. With noise taken into account, the target location is solved as the position that is closest to all the hyper-spheres and hyper-planes formed by all energy ratios in the least square sense, i.e., the single target location is solved by minimizing the following cost function:

$$J(\boldsymbol{\rho}) = \sum_{l_1=1}^{L_1} \left(|\boldsymbol{\rho} - \mathbf{c}_{l_1}| - \zeta_{l_1}\right)^2 + \sum_{l=1_2}^{L_2} \left(\boldsymbol{\iota}_{l_2}^T \boldsymbol{\rho} - \tau_{l_2}\right)^2 \tag{19}$$

Where $L_1 + L_2 = L$, L is the pairs of energy ratios can be computed in our sensor field, l_1 and l_2 are indices of the energy ratios computed between different pairs of sensor energy readings. L_1 and L_2 are the number of hyper-spheres and the number of hyper-planes respectively.

Again, exhaustive search, *MR* search can be used to solve this *NLS* estimation.

C. Sub-band Energy Based Location Estimation

While region-based fusion detection based on the node detection results from *FTE CFAR* detector, *SE CFAR* detector and *MM CFAR* detector can filter out a large amount of false alarms caused by pure strong background noise and therefore, localization algorithm won't be executed by the manager node, there are cases that targets are in the region, but background is noisy. In such cases, localization algorithm will be executed. However, the measured acoustic signals are quite noisy and if we use these signals to perform our energy based localization algorithm, the location results are no longer the true target location. To address this problem, we use sub-band energy to estimate the possible source location candidates and then, use sequential bayesian decision to identify the most probably location candidate.

When signal propagates in the air, signal decay factor may be different at different frequency range. Typically, decay factor for high frequency components of a signal is higher than that for low frequency components. In many real applications, signal is band limited, and the dominant frequency range of a signal is not broad. For example, the dominant frequency range for AAV acoustic signal is between 0HZ and 500HZ. The dominant frequency range for DW acoustic signal is between 0HZ and 200HZ. As a results, we can assume that the decay factor in these dominant frequency range is constant. In our model, we assume that the sub-band energy decay factor is 2 for all the dominant frequency components of the target signal. Another assumption in our sub-band energy based localization is that we assume each frequency component of a signal is independent and won't interfere with each other when propagating in the air. Besides, we assume frequency components of the signal won't be changed by propagating in the air.

Based on above two assumptions, we can use sub-band energy decay model to estimate the target location candidates using different sub-band energies. To do this, we can still use the same energy decay function denoted as equation (1). However, the measurement energy y_i should be replaced by sub-band energy y_{i_k}, source energy S_j is replaced by S_{j_k} and noise energy ξ_i is replaced by ξ_{i_k}. Here y_{i_k} stands for the k^{th} sub-band energy component measured by the i^{th} sensor. S_{j_k} stands for the k^{th} sub-band energy component for j^{th} source. ξ_{i_k} stands for the k^{th} sub-band energy component for noise energy ξ_i. ξ_{i_k} is assumed to be Gaussian distributed with mean μ_{i_k} and variance σ_{i_k}. μ_{i_k} and σ_{i_k} are estimated by the i^{th} sensor node using *SE CFAR* detector.

Using the algorithm described in the previous section for i^{th} sub-band energy decay function, we get target location candidate $\mathbf{\Gamma}_i$ and source sub-band component $\mathbf{SS}_i$ as:

$$\mathbf{\Gamma}_i(n) = [\boldsymbol{\rho}_1^T \ \boldsymbol{\rho}_2^T \ \cdots \ \boldsymbol{\rho}_K^T]_i^T(n) \tag{20}$$

$$\mathbf{SS}_i(n) = [S_{1_i}(n), S_{2_i}(n), ..., S_{K_i}(n)]^T \tag{21}$$

where i denotes the sub-band range i, K stands for number of target sources, and n denotes the time period n.

IV. Location Identification

Using sub-band energy based localization algorithm, we get the target location candidates $\mathbf{\Gamma}_i(n)$ and source sub-band component $\mathbf{SS}_i(n)$ at any time interval n. We would like to identify which location candidate is the most probable target location.

Before we describe the location identification algorithm, we clarify here that in our whole collaborative target detection and localization algorithm, target tracking is an important step. The tracking algorithm is implemented using the standard Kalman filter, which uses the localization results and previous tracking results to predict the target location at the next time step. Note that Kalman filter is a sequential bayesian estimator when we assume that noise is Gaussian.

To identify which sub-band localization result is the most probable target location, we need to separate the situation into two phases. One phase is at the stage that target detection and localization estimation is not guaranteed to be accurate and robust. Therefore, location prediction using Kalman filter which uses the localization results is also not guaranteed to be accurate. We call it as initialization phase. Another phase is the robust phase. At this phase, the localization estimation is robust. Prediction based on the localization results is also robust.

Denote $\mathbf{\Gamma}(n)$ as the identified target location at time n, $\widehat{\mathbf{\Gamma}}(n)$ as the predicted target location from Kalman filter. At the robust phase, we can assume that real target location at time step n is Gaussian distributed with mean $\widehat{\mathbf{\Gamma}}(n)$ and variance $\widehat{\mathbf{\Sigma}}(n)$. Identification of the target location at this robust phase is performed as follows:

$$\mathbf{\Gamma}(n) = \mathbf{\Gamma}_{i^*}(n) \tag{22}$$

Where $i^* = \underbrace{\arg\mathrm{MAX}}_{\{i\}} P(\mathbf{\Gamma}_i(n)|\widehat{\mathbf{\Gamma}}(n))$

The identified target location is then feeded into the Kalman filter. Kalman filter uses this data to predict the target location at the next time step, i.e.,

$$\widehat{\mathbf{\Gamma}}(n+1) = f(\mathbf{\Gamma}\text{(n)} \ \ \mathbf{\Gamma}\text{(n-1)} \ \ ... \ \ \mathbf{\Gamma}\text{(n-L+1)}) \tag{23}$$

where f is the function of Kalman filter. $\widehat{\mathbf{\Sigma}}(n+1)$ is predicted as follows:

$$\widehat{\mathbf{\Sigma}}(n+1) = (1 - \frac{1}{L})\widehat{\mathbf{\Sigma}}(n) + \frac{1}{L}(\widehat{\mathbf{\Gamma}}(n) - \mathbf{\Gamma}(n))(\widehat{\mathbf{\Gamma}}(n) - \mathbf{\Gamma}(n))^T \tag{24}$$

Define:

$$\mathbf{X}(n) = [\mathbf{\Gamma}\text{(n)} \ \ \mathbf{\Gamma}\text{(n-1)} \ \ ... \ \ \mathbf{\Gamma}\text{(n-L+1)}]^T$$

$$\widehat{\mathbf{X}}(n) = \left[\widehat{\mathbf{\Gamma}}(n) \ \ \widehat{\mathbf{\Gamma}}(n-1) \ \ ... \ \ \widehat{\mathbf{\Gamma}}(n-L+1)\right]^T$$

$$R(n) = \frac{1}{A^2}\left(\mathbf{X}(n) - \widehat{\mathbf{X}}(n)\right)^T \left(\mathbf{X}(n) - \widehat{\mathbf{X}}(n)\right)$$

We judge target localization goes into the robust phase if:

$$R(n) \in T_\alpha^2(L)$$

Where α is the confidence level we choose for the T^2 test. A is the accepted error bound for a particular application. For example, in our AAV target localization application, A can be chosen as 30. L is the freedom of χ^2 distribution for R(n).

If $R(n)$ doesn't satisfy above T^2 test, localization algorithm goes into the initial phase. At this phase, the location is identified by trying to find a trajectory from time $n-L+1$ to current time n that will minimize the cost function l, i.e.,

$$[\mathbf{\Gamma}(n), \mathbf{\Gamma}(n-1), ..., \mathbf{\Gamma}(n-L+1)] = \left[\mathbf{\Gamma}_{i_0^*}(n), \mathbf{\Gamma}_{i_1^*}(n-1), ..., \mathbf{\Gamma}_{i_{L-1}^*}(n-L+1)\right] \tag{25}$$

Where $[i_0^*, i_1^*, ..., i_{L-1}^*] = \underbrace{\arg\operatorname{Min}}_{\{i_0, i_1, ..., i_{L-1}\}} \left\{l(\mathbf{\Gamma}_{i_0}(n), \mathbf{\Gamma}_{i_1}(n-1), ..., \mathbf{\Gamma}_{i_{L-1}}(n-L+1))\right\}$

The cost function l is defined as square error function, i.e.:

$$l(\mathbf{\Gamma}_{i_0}(n), \mathbf{\Gamma}_{i_1}(n-1), ..., \mathbf{\Gamma}_{i_{L-1}}(n-L+1)) = \sum_{j=0}^{L-1} l_{i_j}(n-j) \tag{26}$$

Where:

$$l_{i_j}(n-j) = |\mathbf{Z}_{i_j}(n-j) - \widehat{\mathbf{Z}_{i_j}}(n-j)|^2$$

is the square error between the normalized measured sub-band i_j's energy and the sum of decayed sub-band i_j's energy of all sources, assuming the sources sit at the positions estimated from the i_j sub-band energy based localization function, i.e.,

$$\mathbf{Z}_{i_j}(n-j) = \left[\begin{array}{ccc} \frac{y_{1_{i_j}} - \mu_{1_{i_j}}}{\sigma_{1_{i_j}}} & \frac{y_{2_{i_j}} - \mu_{2_{i_j}}}{\sigma_{2_{i_j}}} & \cdots \frac{y_{N_{i_j}} - \mu_{N_{i_j}}}{\sigma_{N_{i_j}}} \end{array}\right]^\Gamma (n-j) \tag{27}$$

$$\widehat{\mathbf{Z}_{i_j}}(n-j) = \mathbf{G}_{i_j}(n-j)\mathbf{D}(n-j)\mathbf{SS}_{i_j}(n-j) \tag{28}$$

Where:

$$\mathbf{G}_{i_j}(n-j) = diag\left[\begin{array}{ccc} \frac{g_1}{\sigma_{1_{i_j}}} & \frac{g_2}{\sigma_{2_{i_j}}} & \cdots \frac{g_N}{\sigma_{N_{i_j}}} \end{array}\right](n-j)$$

$$\mathbf{D_{i_j}}(n-j) = \left[\begin{array}{cccc} \frac{1}{d_{11_{i_j}}^2} & \frac{1}{d_{12_{i_j}}^2} & \cdots & \frac{1}{d_{1K_{i_j}}^2} \\ \frac{1}{d_{21_{i_j}}^2} & \frac{1}{d_{22_{i_j}}^2} & \cdots & \frac{1}{d_{2K_{i_j}}^2} \\ \vdots & \vdots & \ddots & \vdots \\ \frac{1}{d_{N1_{i_j}}^2} & \frac{1}{d_{N2_{i_j}}^2} & \cdots & \frac{1}{d_{NK_{i_j}}^2} \end{array}\right](n-j)$$

$d_{kl_{i_j}}(n-j) = |\boldsymbol{\rho}_{l_{i_j}}(n-j) - \mathbf{r}_k|$ is the Euclidean distance between the k^{th} sensor and the location of l^{th} source estimated by the i_j'th sub-band energy based localization function. $\boldsymbol{\rho}_{l_{i_j}}(n-j) = \mathbf{\Gamma}_{i_j}\{(l-1)p : lp\}(n-j)$, p is the location dimension. $n-j$ stands for the $(n-j)^{th}$ time interval. $\mathbf{\Gamma}_{i_j}$ and $\mathbf{SS}_{i_j}$ are the i_j^{th} location candidate and i_j^{th} source energy component estimated from i_j^{th} sub-band energy based localization algorithm. (See equation 20, 21).

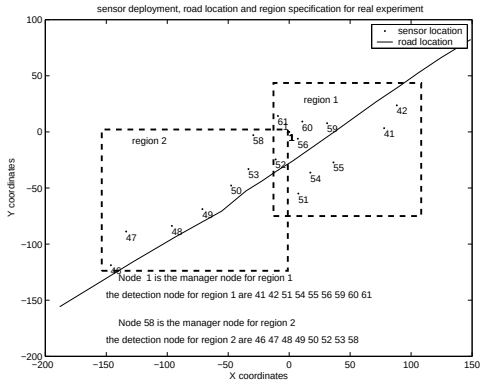

Fig. 4. sensor deployment, road coordinate and region specification for experiments

V. Experiments and Evaluation

A. Sensor Network Configuration

The raw signals were recorded by 29 sensor nodes deployed along the road in the sensor field, CA in November 2001, sponsored by the DARPA ITO SensIT project. Each sensor node is composed of a palm with wireless radio link, an acoustic sensor, a seismic sensor, a PIR sensor and three coaxial cables which connect the sensors to the palm. The data we used to evaluate our collaborative source detection and localization algorithms were taken from 15 sensor nodes recording the acoustic, PIR and seismic signatures of AAV vehicle going from east to west during a time period of 2 minutes. Fig. 4 shows the road coordinates and sensor node positions, both supplied by the global positioning system (GPS). The sensor field is divided into two regions as shown in Fig. 4. Region 1 is composed of node $1, 41, 42, 51, 54, 55, 56, 59, 60, 61$. Region 2 is composed of node $46, 47, 48, 49, 50, 52, 53, 58$. In region 1, node 1 is chosen as manager node, others are detection node. In region 2, node 58 is chosen as manager node, others are detection node. The sampling rate is fs = 4960Hz. The energy is computed by averaging the T=0.75sec non-overlapping data segment (3720 data points).

B. Target Detection and Localization

Fig. 5 and Fig. 6 show the *FTE CFAR*, *SE CFAR*, *MME CFAR* node detection results and final region fusion detection results. The constant C we choose for the *CFAR* detector are $C = [3.5, 3.5, 5, 5, 10, 10]$ for acoustic total energy, sub-band 2, sub-band 1, sub-band 3, seismic and PIR detection respectively. $\alpha = 1/100$ (i.e, average length=100) for all of the three *CFAR* detector. The weights we used for the region fusion decision of the filtered total acoustic energy based detection, acoustic sub-band 2 energy based detection , acoustic sub-band 1 energy based detection, acoustic sub-band 3 energy based detection, seismic energy based detection and PIR energy based detection are 0.3,0.4,0.2,0.1, 0.5, 0.1 respectively. If the region fusion result is bigger than or equal to 0.5, manager node announces the target.

With the fusion of the above three different node detection results, we dramatically decrease the probability of miss detection and fault alarm. Table 1 shows the performance improvement by using the fusion of three detector results in stead of using the acoustic energy based CFAR detector results only. Here, we define sensitivity as the rate of detection when target is in the region. We define specifity as the rate of correct announcement when the region announces the target detection.

Table 1. Sensitivity and Specifity of Target Detection

Target Detection Approach	Region	Sensitivity	Specifity
Acoustic Energy Based CFAR Node Detector + Region Fusion	$Region1$	100	74.6
	$Region2$	64	90
FTE CFAR, SE CFAR, MME CFAR Node Detection + Region Fusion	$Region1$	100	86.3
	$Region2$	89	100

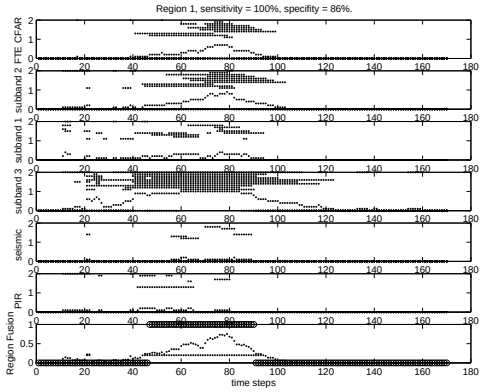

Fig. 5. *FTE CFAR, SE CFAR, MME CFAR* node detection and region fusion detection for region 1 (AAV)

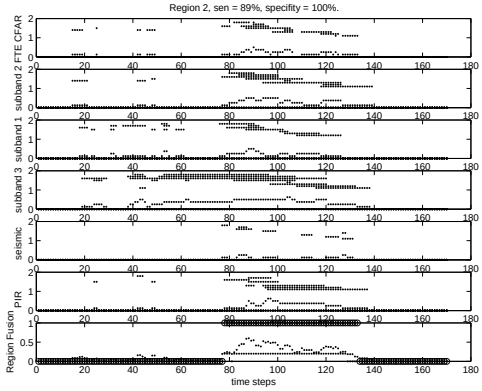

Fig. 6. *FTE CFAR, SE CFAR, MME CFAR* node detection and region fusion detection for region 2 (AAV)

Fig. 7 shows the AAV ground truth and the localization results based on the normal energy based localization (*EBL*) approach and identified sub-band energy based localization approach. *ML* algorithm with projection solution and *MR* search is used for both of the approaches. The search grid size we chose is: 4*4, 2*2, 1*1.

To evaluate this new collaborative source localization algorithm, we compute the localization errors defined as the Euclidian distance between the location estimations and the true target locations. The true target location can be determined since they must be positioned on the target trajectory which can be extracted from GPS log. These localization errors are then grouped into different error range, i.e., $0 \sim 10, 10 \sim 20, ...40 \sim 50, \geq 50$. We call it as error histogram of our localization algorithm. Fig. 8 shows this localization error histogram for AAV localization. Fig. 7 and Fig. 8 show that identified sub-band *EBL* approach greatly improves the performance of localization estimation compared with the normal *EBL* approach in the noisy environment.

C. Discussion

From experiment, we can see that, although the set of data we used is very noisy, the new approach using *FTE CFAR* detector, *SE CFAR* detector, *MME CFAR* detector and region fusion decision based on these three detection results still provides very good performance of target detection. The false alarm and miss detection decrease a lot compared to the region fusion decision based on normal *CFAR* node detection only. Since localization algorithm is executed only when targets are detected in the region, and locations are searched in the detected region which minimize the cost function, decreasing of the miss detection and false alarm increases the localization performance in the sense that localization is searched in the correct region. Meanwhile, sub-band energy based location candidates estimation and location identification from those candidates provide a way to filter out the fault location estimation, and therefore provide better location estimation. These facts

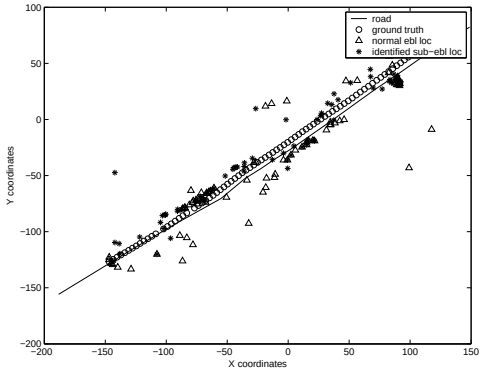

Fig. 7. AAV ground truth and localization estimation results using normal *EBL* approach and identified sub-band *EBL* approaches. *ML* algorithm with projection solution and *MR* search is used for both of the approaches. *MR* search grid size is 4*4, 2*2 and 1*1.

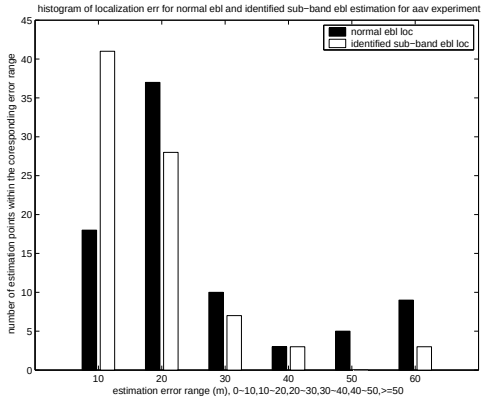

Fig. 8. Estimation error histogram for AAV experiment data

imply that sub-band energy distribution is an important characteristics that can be used to make our detection and localization algorithm more robust in the noisy environment.

In fact, using sub-band energy based target detection and localization is a way of short-time frequency analysis. This is because we separate the signal into different sub-band space. Meanwhile, we use certain time window to calculate these sub-band energies. The algorithm also uses the space information of the sensor network system because the algorithm uses the sensor locations for location candidates estimation. Information of signal variations with time is also used by using the sequential bayesian estimation for identification of the target candidate location. Therefore, this new approach uses almost all the information we have, from short-time sub-band energy component, sensor network space information to signal variation information. Of course, compared to the normal energy based detection and localization algorithm, this new approach need to send more data to the manager node, i.e., its bandwidth is M times of the normal energy based algorithm, where M is the number of sub-band we use. However, this new approach still need relatively less bandwidth compared with other available method since the detection nodes report the data to the manager node only at every time period rather than at every sampling instant.

VI. Conclusion

Sub-band energy based collaborative target localization in wireless sensor network system has been presented. Three steps including target detection, target location candidates estimation and target location identification have been performed to realize the task of target localization. *FTE CFAR* detector, *SE CFAR* detector, *MME CFAR* detector are introduced for node detection. Region based target detection based on these three detection results is provided. Sub-band acoustic energy based algorithm is performed to estimate the target

location candidates when targets are detected in the region. Sequential bayesian estimation is used to identify the most possible target location from these candidate locations.

As discussed in section V-C, this new approach is an approach of short-time frequency analysis. It also uses the space information of the sensor network. Besides, it uses the sequential signal information for the location candidate identification. Therefore, this new approach uses almost all the information we have, from short-time sub-band energy component, sensor network space information to signal variation information.

Experiment has been conducted to evaluate the performance of this new approach for target detection and localization. Results show that this approach decreases a lot of false alarm and miss detection. Therefore, target localization algorithm can be searched in the more correct region. It also improves the performance of target localization compared to the normal energy based localization algorithm.

Sub-band energy based localization need more bandwidth compared to the normal energy based localization algorithm. However, it still needs less communication bandwidth compared to other approach since each sensor reports the data to the manager node only at every time period rather than at every sampling instant. Sub-band we choose for detection and localization is based on the target *PSD* distribution characteristics.

REFERENCES

[1] Estrin, D., Culler, D., Pister, K., and Sukhatme, G.,: Connecting the Physical World with Pervasive Networks, IEEE Pervasive Computing, **1**, Issue 1, (2002), 59-69

[2] Savarese, C., Rabaey, J. M., and Reutel, J.: Localization in distributed Ad-hoc wireless sensor networks, Proc. ICASSP'2001, Salt Lake City, UT, (2001), 2037-2040

[3] Oshman, Y., and Davidson, P., Optimization of observer trajectories for bearings-only target localization, IEEE Trans. Aerosp. Electron., **35**, issue 3, (1999), 892-902

[4] Kaplan, K. M., Le, Q., and Molnar, P.,: Maximum likelihood methods for bearings-only target localization, Proc IEEE ICASSP, **5**, (2001), 3001-3004

[5] Carter G. C.,: Coherence and Time Delay Estimation, IEEE Press, 1993.

[6] Yao, K., Hudson, R. E., Reed, C. W., Chen, D., and Lorenzelli, F.,: Blind beamforming on a randomly distributed sensor array system, IEEE J. Selected areas in communications, **16** (1998) 1555–1567

[7] Reed, C.W., Hudson, R., and Yao,K.,: Direct joint source localization and propagation speed estimation. In Proc. ICASSP'99, Phoenix, AZ, (1999) 1169-1172

[8] Special issue on time-delay estimation, IEEE Trans. ASSP **29**, (1981)

[9] Sheng, X., Hu, Y. H.,: Energy based source localization, to appear IPSN2003.